

PHYTOCHEMICAL, PROXIMATE ANALYSIS AND AN ATTEMPT TO DNA BARCODE AN ENDANGERED MEDICINAL PLANT *BERGENIA CILIATA* (HAW.) STERNB FROM LADAKH IN THE WESTERN HIMALAYAS

RAZA, M.^{1,3*} – MURTAZA, M.² – BANO, S.³ – CHANDRA, R.¹

¹*School of Biotechnology, Shri Mata Vaishno Devi University, Katra 182320, J & K, India*

²*Fermentation & Microbial Biotechnology Division, CSIR-Indian Institute of Integrative Medicine, Jammu 180001, J & K, India*

³*Government Degree College, Kargil 194103, Union Territory of Ladakh, India*

*Corresponding author
email: razabiotek@gmail.com

(Received 25th Jan 2025; accepted 24th Mar 2025)

Abstract. The study investigates the proximate composition and phytochemical properties of an endangered medicinal plant *Bergenia ciliata* from the Western Himalayas to assess its nutritional and medicinal potential. The results showed that the plant has potential antimicrobial and antioxidant activities. DNA barcoding using ITS (internal transcribed spacer) and RBCL (ribulose biphosphate carboxylase large subunit) markers accurately identified and differentiated the species, with ITS providing precise species-level identification and RBCL offering confirmatory data. Moreover, the plant's chemical composition was characterized, highlighting its pharmacological significance. This research contributes to the plant's conservation by authenticating its identity and provides insights into its potential as a medicinal resource. Furthermore, understanding the phyto-constituents offers opportunities to elucidate and discover novel bioactive compounds.

Keywords: *phytochemicals, Ladakh medicinal plants, proximate analysis, antimicrobial, DNA barcoding*

Introduction

Plants possessing therapeutic characteristics are becoming increasingly significant in the food and pharmaceutical sectors due to their ability to prevent and treat diseases (Yu et al., 2021). The utilization of natural products derived from medicinal plants, whether in their pure form or as standardized extracts, offers limitless potential for the advancement of new medications due to the significant abundance of chemical compounds. Throughout history, people have used natural items to effectively treat and heal chronic illnesses like cancer, diabetes, asthma, inflammation, pain, and as substitutes for hormone replacement therapy on a global scale (Rasul, 2018). Lately, both industrialized and developing countries have become increasingly concerned about ensuring the safety, quality, and availability of medicinal plants and herbal treatments. Through the process of standardization and evaluation, herbal medications can contribute to the development of a new era in healthcare by effectively treating human ailments derived from active compounds of plants (Jamshidi-Kia et al., 2017). The pharmaceutical industry, which produces medications primarily derived from plant active compounds, is essential to modern medicine and is frequently utilized as a source of raw materials (Arceusz et al., 2010). However, because the developing world does not have access to synthetic medicine, a significant portion of the world's population

still practices traditional medicine, which is centered on the direct application of medicinal plants because it is an inexpensive practice (Salmerón-Manzano et al., 2020). The pharmaceutical companies primarily use direct collection from the natural habitat to meet the species' demands. Depletion of naturally growing populations due to uncontrolled collection, increasing demand for raw materials, and grazing pressure has resulted in the species becoming extinct with few habitats (Vashistha et al., 2010). In vitro propagation techniques have shown to be a very helpful method for quickly and widely propagating endangered species during the past few decades, helping to preserve the valuable medicinal plant and lessening the risk of extinction (Vashistha et al., 2010). Though the number of plant species in the world is thought to reach 300000, only a small percentage of these can be recognized using conventional methods (Chase and Fay, 2009). Even for specialized taxonomists, accurately classifying and identifying such a vast number of species continues to be a substantial issue. The development of DNA barcoding has improved the classification of biodiversity and recognition (Gregory, 2005). It has been suggested that DNA barcoding is a potent taxonomic appliance for genetic species recognition (Sharma et al., 2020). The nut species in milk beverages was verified through the utilization of DNA barcoding (Ding et al., 2020). Every approach has benefits and drawbacks of its own (Han et al., 2016). Although the morpho-taxonomic method aids in the collection of genuine plant material, applying the same method to processed and powdered materials will prove difficult. Chemical fingerprinting is hampered by the difficulty in establishing species-distinct chemical markers and the sensitivity of the markers to the season, age, and location of plant material compilation (Li et al., 2008). With the development of technology, a sharp decline in the cost of sequencing, and an increase in the diversity of reference sequences, DNA barcoding has become a more reliable and adaptable technique for molecular species identification, which is used to authenticate herbal items and raw pharmaceuticals (Nithaniyal et al., 2017). DNA barcoding makes use of markers that are divergent between specimens but conserved within specimens, making it possible to obtain species-specific sequences with just one set of universal primers. In order to improve conservation, taxonomy, environmental protection, and biodiversity assessment. DNA barcoding can be utilized for specimen explanation, cryptic specimen recognition, and specimen's composition comprehension in biodiversity hotspots (Gill et al., 2019). High levels of inter specific divergence are demonstrated by the ITS spacer, a potent phylogenetic marker at the species level (Álvarez et al., 2003). Due to extensive research on ITS's superior discriminatory ability over plastid regions at low taxonomic levels, it has also been proposed as a plant barcode (Kress et al., 2005), particularly for parasitic plants that provide less resolution than plastid barcodes (Hollingsworth et al., 2011).

Gene *rbcL* is frequently used in phylogenetic analyses, and Genbank contains over 500,000 sequences. This gene has the benefit of being an excellent DNA barcoding region for plants at the family and genus levels, and it is simple to amplify, sequence, and align in the majority of terrestrial plants. But *rbcL* sequences are slow to evolve among plastid genes in flowering plants, this locus has the lowest divergence (Kress et al., 2005). Consequently, because of its weak selective strength, it is inappropriate at the species level (Chen et al., 2010).

High-altitude forage species that have historically been employed are nutrient-rich and can be suggested as a component of nutrient for livestock animals (Kumar et al., 2022). In addition to being used medicinally, medicinal herbs may also be utilized as dietary

supplements (Radha et al., 2021). DNA barcoding identified approximately 20% of the raw medications as contaminated, and that at least 6% of them were from plants with entirely distinct hazardous or therapeutic attributes. It was shown that raw medications, such as powders, dried roots, and entire plants, were more likely to be adulterated than rhizomes, fruits, and seeds (Nithaniyal et al., 2017). *Meconopsis aculeate* Royle (Family: *Papaveraceae*), a significant medicinal herb found in the Himalayan region, can be expanded for use in other industrial applications and demonstrates the highest concentration of bioactive components in medium-polarity solvents (Bahukhandi et al., 2019). Phytochemistry of various *M. esculenta* extracts that revealed the presence of polysaccharides, alkaloids, flavonoids, glycosides, saponins, and tannins. The herb is quite effective in treating ENT infections, diarrhea, anemia, pyrexia, ulcers, and coughs (Shah et al., 2021). The biochemical makeup of medicinal plants and their therapeutic efficacy are regulated by the conditions under which they are grown. These changes and ultimately the survival of medicinal plants is undoubtedly caused by the different biotic and abiotic pressures that are present in the environment across the altitudinal gradient (Jamwal et al., 2023). DNA barcoding method can accurately identify the medicinal plant *Trillium govanianum* and prevent its adulteration with *Paris polyphylla*. The method ensures the correct identification of market samples, helping to maintain product quality, prevent illegal trade, and support sustainable harvesting from natural habitats (Islam et al., 2021). While exploring edible plants, five wild edible plants from the western Himalayas were reported, revealing *Allium rubellum* as the most nutritionally rich. The plants exhibited significant antioxidant and antibacterial properties, particularly *Rheum emodi* and *Stellaria aquatic* (Thakur et al., 2022).

Bergenia ciliata, commonly known as *Pashambeda* (In Ayurveda) or Elephant's Ears, is native to the mountainous regions of Asia. It is predominantly found in the Himalayan region, including parts of India, Nepal, Bhutan, and northern Pakistan. Thriving in alpine and subalpine environments, *Bergenia ciliata* prefers rocky, well-drained soils at elevations ranging from 2000 to 3000 m above sea level. The current study on *Bergenia ciliata* focuses on parameters of its proximate, phytochemical, antioxidant, antimicrobial activities along with identification attempt of the plant via barcode markers for its exact identification to avoid adulteration in formulation prepared from the plant.

Materials and methods

Collection and identification of plant material

The whole plant of *Bergenia ciliata*, collected during its flowering season from July to October in 2023 from Archo La Kargil, Ladakh, India, and its specimen submitted to Biodiversity Centre University of Ladakh under voucher number: LAD-527 and taxonomically identified as *Bergenia ciliate* (Haw.) Sternb. This herbaceous medicinal plant, which belongs to the family *Asteraceae*, is extensively used in Ayurveda for its anti-cancerous, anti-inflammatory, and analgesic properties. The roots and leaves of the plant have been utilized for medicinal purposes. The roots were washed thoroughly in running tap water, then dipped in sterile double-distilled water for 10 min, followed by surface sterilization with 5% sodium hypochlorite for 4-5 min and washing with 70% ethanol for 1-2 min. To remove traces of ethanol, further immersion in distilled water was performed. The effectiveness of the surface sterilization procedure was validated by culturing the final wash onto nutrient agar plates; any bacterial growth on the control plates would indicate inadequate surface sterilization (*Fig. 1*).



Figure 1. Plant sample from Western Himalayas

Proximate analysis

Extraction using Soxhlet

Moist extraction was done for better outcome using Soxhlet. Briefly, Dried 5 g of sample was weighed, placed in a cheese cloth and kept in thimble. The solvent methanol was used for extraction. Solvent was added to a round bottom flask, which was attached to a Soxhlet extractor and condenser. The crushed plant material was loaded into the thimble, which was then placed inside the Soxhlet extractor. The solvent was heated using the heating mantle as the solvent boils, vapor starts to rise to extraction chamber, moving through the apparatus to the condenser. The condensate then drips into the reservoir containing the thimble. Once the level of solvent reached the siphon it was poured back into the flask and the cycle begins again. The process ran for a total of 6 h. The extract was used for re-extraction twice with fresh 5 g powder each time using same process. The collected extract was concentrated using a rotary evaporator to dryness and then weighed. Yield was then calculated from the extract.

Moisture content

Pre-weight of the glass plate was taken by using weighing balance. After that, 2 g of the sample was measure and took the combined weight (W1). Then, sample was placed in oven for 30 min at 100°C. After 30 min stop the drying process, then the weight of the glass plate with sample was taken. Then, the % moisture content of the sample was calculated using *Equation 1*.

$$\text{Moisture content (\%)} = \frac{W2 - W3}{W2 - W1} \times 100 \quad (\text{Eq.1})$$

W2 = mass, in g, of the petri dish and sample before drying; W3 = mass, in g, of the petri dish and sample after drying; W1 = mass in g of the petri dish.

Ash content

Clean and labeled crucibles was placed in a muffle furnace at 600°C for 1 h. Turnoff the furnace and transfer partially cooled crucibles into a desiccators and cool to room temperature. Weigh crucible quickly to prevent possible moisture absorption. Weigh 2 g of dry food into the pre-weighed crucible. Crucible was placed in muffle furnace at 550°C for 12–18 h. Organic material was burn off until the samples become completely free from carbon and appear as light gray or white ash. Temperature was raised to 600°C and leave 1–2 h depending on the incompleteness of the ashing (Sarma et al., 2020). Ash content is calculated using the formula as in *Equation 2*.

$$\text{Ash content} = \frac{(M2-M1)}{M} \times 100 \quad (\text{Eq.2})$$

M2 = mass in g of crucible ash; M1 = mass in g of crucible; M = mass in g of sample.

Crude fiber content

The Crude fiber content was estimated by the Acid-Alkali digestion method as suggested by standard AOAC protocols (Adetunji et al., 2023). 5 g sample (Ws) were added into 200 ml of 1.25% of H₂SO₄ and boiled for 30 min. This solution and the content was then poured into Buchner funnel containing the muslin cloth. The residue obtained was then kept into 200 ml 1.25%NaOH solution and boiled for 30 min. This content was again transferred to the Buchner funnel and filtered. The residue this time was washed twice with 75% alcohol and thrice with petroleum ether. The final residue obtained was placed into a clean dry crucible and the total weight was taken as W1. The content was dried in the hot air oven at 110°C for 2 h to a constant weight. The dried crucible was removed, cooled and its weight was taken as W2. Then, difference in weight (i.e. loss in ignition) was recorded and the calculation was done using the given formula as in *Equation 3* and expressed in percentage crude fiber.

$$\text{Crude Fibre content \%} = \frac{W1 - W2}{Ws} \times 100 \quad (\text{Eq.3})$$

Crude fat content

For estimation of crude fat content, 2 g of sample (Ws) was taken and kept in the pre-weight conical flask (W1). 40 mL of diethylether was added to the flask. Raise the heaters into position. Leave about a ¼ inch gap between the flask and the heating element. After extraction, allow the ether to drain out for 30 min. Distill until a thin layer of ether remains in the bottom of the flask, and then lower the heater. Do not allow to flask to boil dry. Overheating will oxidize the fat. Cool in a desiccators and weigh and record weight (W2) (Shin and Park, 2015). The percentage crude fat is calculated by using *Equation 4*.

$$\text{Crude fat \%} = \frac{W2 - W1}{Ws} \times 100 \quad (\text{Eq.4})$$

Total protein

The protein content of samples was estimated by the Kjeldahl method (Bathe et al., 2012), where the sample was kept for acidic digestion followed by neutralization and

finally the titration. 5 g of samples was introduced in digestion flask and to that 10 ml of concentrated H₂SO₄ and 5 g of digestion mixture of K₂SO₄:CuSO₄:Na₂SO₄ (equal ratio) was added. The flask was swirled in order to mix the contents thoroughly placed on heater to start digestion till the mixture become clear (blue green in color). It took 3 h to complete the process. The digest was cooled and transferred to 100 ml volumetric flask. The volume was topped up to mark using distilled water. Then from those ten milliliters of the digest was introduced in the distillation tube where 10 ml of 0.5 N NaOH was gradually added. Distillation continued for 10 min and NH₃ (Ammonia gas) produced was collected as NH₄OH (Ammonium hydroxide) in a conical flask containing 20 ml of 4% boric acid solution with a drop of modified methyl red indicator. During distillation yellowish color appeared due to NH₄OH. The distillate was then titrated against standard HCL solution of 0.25 mol/L concentration till a pink color observed. At this step the initial and final reading were noted to calculate the amount of titrant used and noted as Vs. A blank was also run as previous to the sample and for the blank nitrogen content of acetanilide or tryptophan after addition of 1 g of saccharose was determined at the titration step and the volume of titrant used was noted as Vb. The %N in samples was calculated via the given formula followed by the calculation of % P by multiplying the %N with the protein factor (PF) that is 6.25. The percentage nitrogen and protein is calculated using *Equations 5 and 6*, respectively.

$$\%N = \frac{Vs - Vb \times F \times C \times f \times M(N)}{m \times 1000} \times 100 \quad (\text{Eq.5})$$

where: Vs- volume of titrant used for sample; Vb- volume of titrant used for blank; F- molar reaction factor of titrant (HCl-1 and H₂SO₄- 2); C- concentration of titrant (mol/L) = 0.25 mol/L; f- Factor of titrant = 1; M(N)- Molecular weight of Nitrogen = 14.007g/mol; m- sample weight; 1000- conversion factor (ml into L); %N- % weight of N.

$$\%Protein = \%N \times Protein\ Factor(6.25) \quad (\text{Eq.6})$$

Carbohydrate estimation

The carbohydrate content was estimated by anthrone method (Yemm and Willis, 1954). Briefly a standard glucose plot was prepared with step as- pipetted out into a series of test tubes in different volumes of glucose solution from the stock solution (10 mg/ml) and make up the volume with distilled water. To each tube added 5 mL of the anthrone reagent (supplied) and mixed well by vortexing. Cooled the tubes. Covered the tubes with Caps on top and incubate at 90°C for 15 min or boiling water bath for 10 min. Cooled to room temperature and measured the optical density at 620 nm against a blank. Prepared a standard curve of absorbance vs. glucose concentration. Calculated the amount of carbohydrate in the sample using standard calibration graph.

Antimicrobial activity

The antimicrobial activity of crude extract (BR) was tested using the microdilution method, employed according to CLSI (Clinical and Laboratory Standards Institute) guidelines. The stock solution of extract BR was prepared at a concentration of 10 mg/mL in DMSO. Two-fold serial dilutions of this stock solution were made in a 96-

well U-bottom microtiter plate, ranging from 64 to 512 µg/mL. Positive control wells contained ciprofloxacin, while negative controls had only DMSO. Bacterial suspensions of *Escherichia coli*, *Pseudomonas aeruginosa*, *Bacillus subtilis*, *Staphylococcus aureus*, *Micrococcus luteus*, and *Candida albicans* were prepared and adjusted to a 0.5 McFarland standard. These suspensions were inoculated into the wells, achieving a final concentration of 1×10^5 CFU/mL. The plates were incubated at 37°C for 24 h for bacterial strains and at 28°C for 48 h for *Candida albicans*. After incubation, the minimum inhibitory concentration (MIC) of extract BR was determined by identifying the lowest concentration at which visible growth was inhibited. This MIC value was compared to that of the positive control to evaluate the antimicrobial effectiveness of extract BR.

Antioxidant activity using DPPH (1,1 diphenyl 2 picrylhydrazyl)

The antioxidant activity of the crude extracts was performed using DPPH-based scavenging activity assay. The 0.53 mg DPPH (Sigma-Aldrich, New Delhi, India) was added to 10 mL of methanol (HiMedia Laboratories, Mumbai, India) to measure the activity of the (200 µg/mL) extracts in flat-bottom 96-well plates. The plate was incubated for 30–45 min in the dark, and the absorbance was measured at 517 nm in a multimode microplate reader (Tecan Infinite 200 pro, Austria). The scavenging activity of the antioxidants is based on the reduction of DPPH (a stable free radical) with strong absorbance at 517 nm, giving a deep violet color. The absorption decreases as the free radical gets a hydrogen donor and DPPH is reduced to DPPH-H,

which leads to decolorization (yellow color). Ascorbic acid was used as a positive control. The percentage of DPPH radical scavenging activity was expressed as the decrease in absorbance percentage of the samples compared to the control (DMSO + DPPH) as shown in Equation 7.

$$\% \text{ DPPH inhibition} = \frac{\text{Absorbance of control} - \text{Absorbance of sample}}{\text{Absorbance of control}} \times 100 \quad (\text{Eq.7})$$

Phytochemical analysis

Preparation and analysis of plant samples using inductively coupled plasma mass spectrometry (ICP-MS)

The sample preparation process involves dissolving plant material to analyze heavy metals using ICP-MS. Initially, 1 gram of plant sample is placed in a test tube, to which 15 ml of nitric acid (HNO₃) and 5 ml of perchloric acid (HClO₄) are added. The mixture is left overnight in a fume cupboard for thorough dissolution. The next day, the mixture is heated on a stove starting at 90°C, with the temperature increased by 10°C every 2 min until it reaches 170°C. At this temperature, hydrogen peroxide (H₂O₂) is added dropwise until a white fume indicates complete reaction. The mixture is then cooled and diluted to 50 ml with deionized water in a volumetric flask. Afterward, the solution is filtered through Whatman no. 42 filter paper. For heavy metal analysis, the resulting solutions are analyzed using an ICP-MS, specifically a Perkin Elmer NexION1000. The ICP-MS is operated with specific conditions including argon plasma gas flows, lens voltage, and RF power. The analysis is performed with a peak hop acquisition mode, where one point per mass is recorded at maximum peak, with each reading consisting of 8 sweeps and 6 runs, ensuring accuracy through rinse time and solution protocols.

Fourier-transform infrared (FTIR) spectroscopy

The Rotavapour dried methanolic extract sample of *Bergenia* species was analyzed using Attenuated Total Reflectance Fourier Transform Infrared (ATR-FTIR) spectroscopy. The analysis was performed with the IRaffinity-1S instrument (Serial No: A221359, Shimadzu, Japan). Spectra were collected at room temperature with a resolution of 2 cm^{-1} over the range of $4000\text{--}600\text{ cm}^{-1}$. The total collection time was approximately 5 min, with each spectrum obtained using 16 scans.

Gas chromatography–mass spectrometry (GC-MS) analysis

The GC-MS analysis of the methanolic extract of *B. ciliata* was conducted using a Perkin Elmer Autosystem XL equipped with a TurboMass detector and a $30\text{ m} \times 0.25\text{ mm} \times 0.25\text{ }\mu\text{m}$ column. The oven temperature was initially set at 75°C for 5 min and then gradually increased to 280°C . A $2\text{ }\mu\text{l}$ aliquot of the extract was injected in split mode. Helium was used as the carrier gas, flowing at a rate of 1 ml/min. The compounds in the extract were identified by analyzing the GC retention times, and major peaks were confirmed by comparing the mass spectra with the National Institute of Standards and Technology (NIST) database.

Molecular analysis for DNA barcoding

Molecular analysis was performed at DBT-Rajeev Gandhi centre for Biotechnology, Kerala, India. The barcoding method involves genomic DNA extraction, DNA amplification, and DNA sequencing, and taxonomic identification against available DNA banks.

The genomic DNA isolation was carried out by using plant genomic DNA isolation kit- NucleoSpin® Plant II Kit. Liquid nitrogen is used to homogenize about 100 mg of the tissue, and the granulated tissue is then placed into a microcentrifuge tube. After adding 400 microliters of buffer PL1, vortexing for 1 min. After adding and mixing, ten microliters of RNase A solution are inverted. For 10 min, the homogenate is incubated at 65°C . After being moved to a Nucleospin filter, the lysate is centrifuged for 2 min at $11000 \times g$. The filter is disposed of once the liquid flow through it has been collected. After adding and thoroughly mixing, 450 microliters of buffer PC are added. After the sample is moved to a Nucleospin Plant II column and centrifuged for 1 min, the liquid that flows through is disposed off. The column is filled with 400 microliters of buffer PW1, centrifuged for 1 min at $11000 \times g$, and the liquid that flows through is disposed of. Next, add 700 μl of PW2, centrifuge at $11000 \times g$, and dispose of the liquid phase. To dry the silica membrane, 200 μl of PW2 is included and centrifuged at $11000 \times g$ for 2 min. After moving the column to a fresh 1.7 ml tube, 50 μl of buffer PE is included, and it is maintained for 5 min at 65°C . The DNA is then extracted from the column by centrifuging it for 1 min at $11000 \times g$. The eluted DNA is then stored at 4°C .

Agarose gel electrophoresis for DNA quality check

The use of agarose gel electrophoresis allowed for the standard assessment of the isolated DNA. 5 μl of DNA, mixed with 1 μl of 6X gel-loading buffer (0.25% bromophenol blue, 30% sucrose in TE buffer pH-8.0). Samplings were placed onto a 0.8% agarose gel that was readied in a 0.5X Tris-Borate-EDTA (TBE) solution that contained 0.5 μg of ethidium bromide per milli-liter. 0.5X TBE is used as the

electrophoresis buffer, and the gel is electrophoresed at 75 V until the bromophenol dye front moved to the bottom. The gels were seen in a UV transilluminator (Genei), and a Gel documentation system (Bio-Rad) is utilized to take the picture over a UV lamp.

PCR analysis and primers employed for PCR amplification profile of ITS and rbcl

The PCR analysis for amplifying the *ITS* and *rbcl* region were conducted using PCR kit (Macherey-Nagel). A reaction mix comprising 5 μ L of 2X Phire Master Mix, 4 μ L of purified water (D/W), 0.25 μ L of forward primer, 0.25 μ L of reverse primer, and 1 μ L of DNA template and the primer sequences are as shown in *Table 1*. The PCR thermal cycler was set to a primary denaturation step at 98°C for 30 s, pursued by 40 cycles of 98°C for 5 s, 58°C for 10 s, and 72°C for 15 s. The terminal extension was performed at 72°C for 60 s, and the reaction was held at 4°C indefinitely to maintain the amplified DNA. This protocol ensured the successful amplification of the *ITS* region for subsequent sequencing and analysis.

Table 1. Primers used

Target	Primer name	Direction	Sequence (5' \rightarrow 3')
<i>ITS</i>	ITS-F2	Forward	GATTGAATGATCCGGTGAAG
	ITS-R2	Reverse	CTCGCCGTTACTAGGGGAAT
<i>rbcl</i>	RBCL-AF	Forward	ATGTCACCACAAACAGAGACTAAAGC
	RBCL-724R	Reverse	TCGCATGTACCTGCAGTAGC

Agarose gel electrophoresis of PCR products

1.2% agarose gels readied in 0.5X TBE buffer consisting of 0.5 μ g/ml ethidium bromide were employed to check the PCR products. A UV transilluminator (Genei) is used to visualize the gels, and an image snapped ver UV light utilizing a Gel documentation system (Bio-Rad) then used to load 1 μ l of 6X loading dye with 4 μ l of PCR products and electrophoresis is carried out at 75V energy source with 0.5X TBE as the electrophoresis buffer for approximately 1-2 h, till the bromophenol blue front had moved to the bottom of the gel.

ExoSAP-IT treatment

The hydrolytic enzymes Exonuclease I and Shrimp Alkaline Phosphatase (SAP) are combined in ExoSAP-IT (GE Healthcare) to eliminate undesired primers and dNTPs from a PCR product mixture without interfering with subsequent applications.

After combining five microliters of PCR product with 0.5 μ l of ExoSAP-IT, the mixture is maintained for 15 min at 37°C, and then the enzyme is inactivated for 5 min at 85°C.

Sequencing using BigDye Terminator v3.1

Employing the BigDye Terminator v3.1 Cycle sequencing Kit (Applied Biosystems, USA) and the manufacturer's guidelines, the sequencing reaction is taken out in a PCR thermal cycler (GeneAmp PCR System 9700, Applied Biosystems).

The ingredients made up the sequencing PCR mix are as in *Table 2*.

Table 2. PCR mix components

D/W	6.6 μ L
5X Sequencing buffer	1.9 μ L
Forward primer	0.3 μ L
Reverse primer	0.3 μ L
Sequencing mix	0.2 μ L
Exosap treated PCR product	1 μ L

The sequencing PCR mix included 6.6 μ L of D/W, 1.9 μ L of 5X Sequencing Buffer, 0.3 μ L each of forward and reverse primers, 0.2 μ L of Sequencing Mix, and 1 μ L of ExoSAP-processed PCR product. The sequencing PCR was taken out with a primary denaturation at 96°C for 2 min, pursued by 30 cycles of 96°C for 30 s, 50°C for 40 s, and 60°C for 4 min, with a hold at 4°C indefinitely.

Post sequencing PCR clean up

A clean-up mix was prepared with 5 μ L of D/W, 1 μ L of 3M Sodium Acetate, 0.1 μ L of EDTA, and 44 μ L of 100% Ethanol. Fifty microliters of the mix were included to every well in the sequencing plate consisting of the sequencing PCR product, agitated, and maintained at room temperature for 30 min. The plate was twirled at 3700 rpm for 30 min, the liquid phase decanted, and 50 μ L of 70% ethanol included to every well. The plate was twirled at 3700 rpm for 20 min, and the liquid phase decanted. This wash was repeated, and the sediment was air-dried. The cleaned-up product was sequenced utilizing an ABI 3500 DNA Analyzer.

Sequence analysis

Applied Biosystems' Sequence Scanner Software v1 is utilized to verify the sequence standard. Geneious Pro v5.1 is employed for sequence alignment and any essential adjustment of the obtained sequences.

Results

Proximate analysis

The proximate analysis was done using standard methods as described in the materials and methods section. The medicinal plant showed promising ash content of 4.618%, that corresponds to higher mineral elements. Despite of fleshy leaves the moisture content was also minimal at around 12.917% which means the plant can be stored for larger point of time and will not perish. This provides an advantage that the plant can be used for longer time as traditional medicine without using any preservatives. The plant has sufficient carbohydrate percentage of 75.925% and can be a stable source as a nutritive component in addition to its therapeutic potential in the traditional medicine. Considerable amount of fiber content is reported as well, with 4.19% per gram of sample material taken. This further increases its importance as a therapeutic material for ailments like constipation in the traditional medicine. Therefore, the plant *Bergenia ciliata* carries sufficient potential as a food source in addition to its therapeutic application. *Table 3* depicts the results for proximate analysis showing values for various parameters.

Table 3. Results showing proximate analysis of *Bergenia ciliata*

S.No.	Test	Results/observation
1	Total protein (%)	6.407 ± 0.475
2	Moisture (%)	12.917 ± 0.925
3	Crude fiber (%)	4.199 ± 0.893
4	Crude fat (%)	0.611 ± 0.071
5	Ash (%)	4.618 ± 0.641
6	Carbohydrate (%)	75.925 ± 0.385

Antimicrobial activity

Methanolic extract of *Bergenia ciliata* exhibit notable antimicrobial activity due to their rich bioactive compounds like phenolics, flavonoids, and silica. The extract disrupts microbial cell walls and membranes, making it effective against various bacteria and fungi, with potential applications in natural antimicrobial agents. Finally, the extract is a sustainable, eco-friendly solution for microbial control in medicine, agriculture and food preservation, with ongoing research needed to optimize their use (Fig. 2).

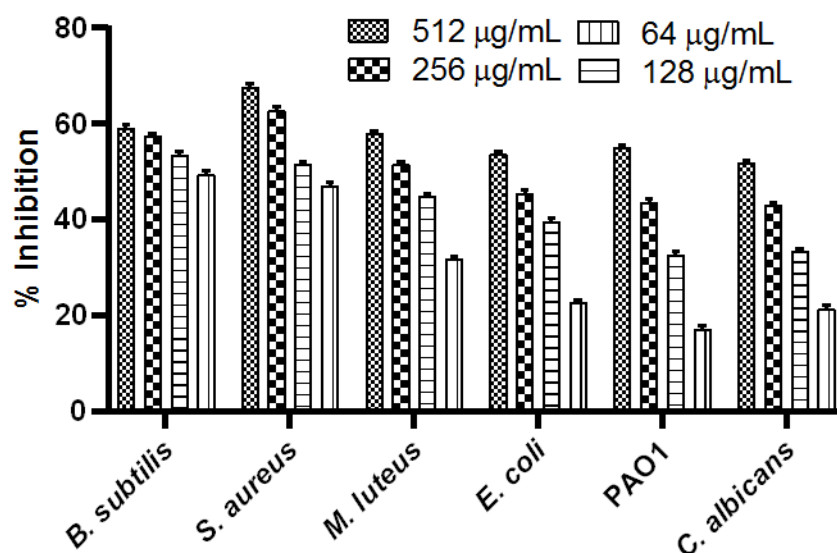


Figure 2. Percentage inhibition of the screened pathogens against *Bergenia ciliata* methanolic extract

The antimicrobial activity of the extract demonstrates significant efficacy, particularly against *Staphylococcus aureus*, with an inhibition rate of $67.74 \pm 0.59\%$ at a concentration of $512 \mu\text{g/mL}$, and a MIC of $256 \mu\text{g/mL}$. Additionally, the extract exhibits notable inhibitory effects against various other microorganisms: *Bacillus subtilis* ($59.17 \pm 0.72\%$), *Micrococcus luteus* ($57.88 \pm 0.66\%$), *Pseudomonas aeruginosa* ($54.99 \pm 0.53\%$), *Escherichia coli* ($53.61 \pm 0.55\%$), and *Candida albicans* ($51.84 \pm 0.55\%$) at the same concentration of $512 \mu\text{g/mL}$. Figure 3 provides the graphical representation of the antimicrobial activity. Table 4 provides data showing that the antimicrobial activity of the extract is potent but decreases as the concentration is reduced.

Table 4. Antimicrobial activity of the methanolic extract of *Bergenia ciliata* against various pathogenic strains

Pathogens	Concentration ($\mu\text{g/mL}$)			
	512	256	128	64
	% Inhibition			
<i>B. subtilis</i>	59.17 \pm 0.72	57.35 \pm 0.57	53.45 \pm 0.65	49.55 \pm 0.61
<i>S. aureus</i>	67.74 \pm 0.59	62.84 \pm 0.82	51.51 \pm 0.63	46.96 \pm 0.72
<i>M. luteus</i>	57.88 \pm 0.66	51.58 \pm 0.54	44.85 \pm 0.64	31.84 \pm 0.48
<i>E. coli</i>	53.61 \pm 0.55	45.49 \pm 0.64	39.64 \pm 0.59	22.67 \pm 0.66
PAO1	54.99 \pm 0.53	43.48 \pm 0.81	32.55 \pm 0.72	17.28 \pm 0.59
<i>C. albicans</i>	51.84 \pm 0.55	42.48 \pm 0.66	33.59 \pm 0.44	21.58 \pm 0.69

Antioxidant activity

Methanolic extract of *Bergenia ciliata* exhibit strong antioxidant activity due to their high content of phenolic compounds, flavonoids, and lignins. These bioactive molecules neutralize free radicals, reducing oxidative stress and protecting cells from damage. The plant's antioxidants contribute to its potential in preventing diseases linked to oxidative stress, such as cancer and cardiovascular disorders. The plant offers promising natural sources for antioxidants, with potential applications in health, food preservation, and cosmetics (Table 5).

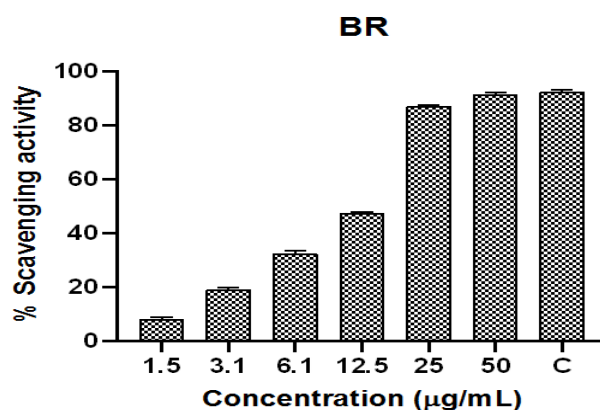


Figure 3. Graphical representation of antioxidant activity of *Bergenia ciliata* methanolic extract

Table 5. Antioxidant activity of *Bergenia ciliata* methanolic extract

Concentration ($\mu\text{g/mL}$)	% activity
1.56	7.96 \pm 0.88
3.125	18.86 \pm 0.72
6.15	32.26 \pm 0.99
12.5	47.29 \pm 0.59
25	86.96 \pm 0.64
50	91.39 \pm 0.66
Ascorbic acid (C)	92.44 \pm 0.55

IC50 = 17.8765

ICP-MS analysis

Table 6 presents the concentration of different elements in the selected plant *Bergenia ciliata*.

Table 6. Concentration of different elements in the selected plant *Bergenia ciliata*

S.No	Element	Concentration in ug/L
1	Na	214.568
2	K	20931.620
3	Ca	3188.875
4	Mg	5898.360
5	Zn	23.571
6	Cu	20.749
7	Mn	46.527
8	Fe	527.579

FTIR spectrum analysis

The FTIR analysis revealed the presence of several functional groups in the *Bergenia* extract. The Figure 4 displays the infrared (IR) spectrum, where transmittance is plotted against wavenumber (cm^{-1}). The x-axis represents the wavenumber which ranges from 4000 cm^{-1} to 400 cm^{-1} , covering the range of IR radiation frequencies. The y-axis measures the percentage of IR light transmitted through the sample, with values ranging from 0% to 100% transmittance. High transmittance values (peaks) suggest less absorption of IR light at these wavenumbers, whereas low transmittance values (troughs) indicate significant absorption.

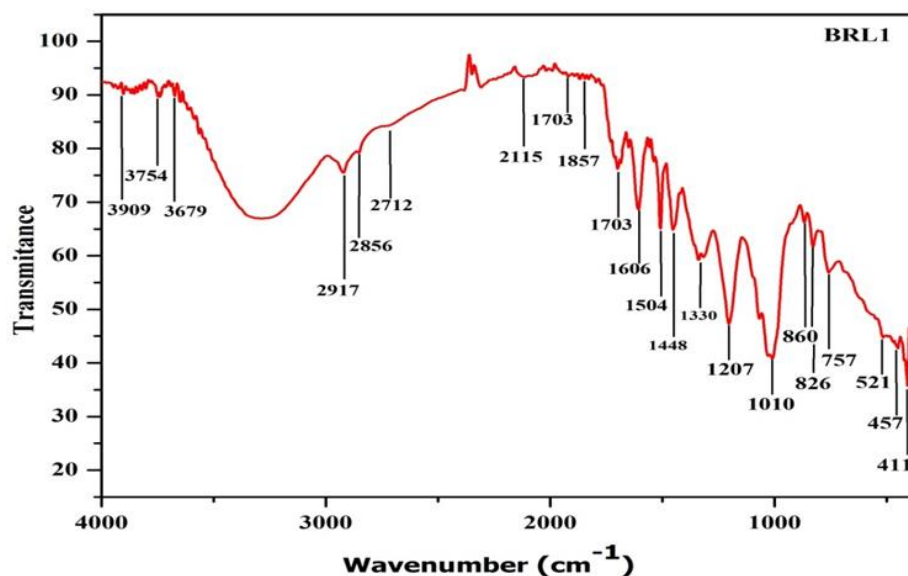


Figure 4. Graphical representation of IR spectrum

Table 7 presents various IR absorption frequencies (in cm^{-1}) that correspond to specific molecular vibrations, along with their associated intensity, functional groups,

and compound classes. For instance, absorption at 3675.42 cm^{-1} and 3629.13 cm^{-1} falls within the $3700\text{-}3584\text{ cm}^{-1}$ range, indicating medium, sharp O-H stretching vibrations typical of alcohols. The frequency 1734.04 cm^{-1} is associated with a strong C = O stretch found in esters, while 1700.28 cm^{-1} and 1683.89 cm^{-1} represent strong C = O stretching in conjugated aldehydes and acids, respectively. The 1653.02 cm^{-1} frequency corresponds to a medium C = C stretch in alkenes. Strong N-O stretching vibrations, characteristic of nitro compounds, are observed at 1558.51 cm^{-1} , 1539.22 cm^{-1} , and 1507.40 cm^{-1} . Lastly, a strong C-F stretch, typical of fluoro compounds, is detected at 1203.00 cm^{-1} . These frequencies and their corresponding vibrations help identify functional groups and determine the compound class in molecular analysis.

Table 7. Detailed spectral data of FT-IR analysis showing functional groups in *Bergenia ciliata*

Frequency cm^{-1}	Reference frequency range	Intensity	Group	Compound class
3675.42	3700-3584	Medium, sharp	O-H stretch	Alcohol
3629.13	3700-3584	Medium, sharp	O-H stretch	Alcohol
1734.04	1750-1735	Strong	C = O Stretch	Esters
1700.28	1710-1685	Strong	C = O stretching	Conjugated aldehyde
1683.89	1710-1680	Strong	C = O stretch	Conjugated acid
1653.02	1658-1648	Medium	C = C stretch	Alkene
1558.51	1600-1300	Strong	N-O stretch	Nitro compound
1539.22	1550-1500	Strong	N-O stretch	Nitro compound
1507.40	1420-1330	Strong	N-O stretch	Nitro compound
1203.00	1400-1000	Strong	C-F stretch	Fluoro compound

GC-MS analysis

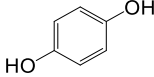
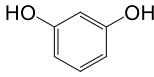
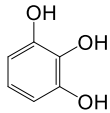
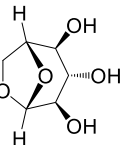
GC-MS analysis of *Bergenia ciliata* identifies the plant's diverse bioactive compounds, such as phenolic acids, flavonoids, and terpenoids. These compounds are responsible for the plant's therapeutic properties, including antioxidant, anti-inflammatory, and antimicrobial activities. The analysis offers a detailed chemical profile, aiding in the understanding of its medicinal potential and applications in traditional remedies and modern pharmaceuticals.

Table 8 presents the results of a GC-MS analysis of *Bergenia ciliata*, detailing the retention times (RT), relative abundance (Area%), mass-to-charge ratios (m/z), molecular formulas, and identified compounds. Four key compounds were detected: Hydroquinone (RT 14.26, 34.24% area) and Resorcinol (RT 13.79, 21.15% area), both with a molecular formula of $\text{C}_6\text{H}_6\text{O}_2$ and an m/z of 110, indicating their similar structural characteristics. The analysis also identified 1,2,3-Benzenetriol (RT 15.51, 20.84% area) with an m/z of 128 and molecular formula $\text{C}_6\text{H}_6\text{O}_3$, and β -D-Glucopyranose, 1,6-anhydro (RT 17.69, 14.42% area) with an m/z of 162 and molecular formula $\text{C}_6\text{H}_{10}\text{O}_5$.

The mass spectra obtained from GC-MS analysis of four compounds are enclosed in the Appendix: Hydroquinone Resorcinol 1,2,3-Benzenetriol and β -D-Glucopyranose, 1,6-anhydro. Each spectrum displays the mass-to-charge ratio (m/z) on the x-axis and the relative abundance of detected ions on the y-axis. For Hydroquinone and

Resorcinol, prominent peaks are observed at m/z values of 53, 55, 81, and 111, with the peak at m/z 111 corresponding to the molecular ions of these compounds (C₆H₆O₂). The spectrum for 1,2,3-Benzenetriol shows key peaks at m/z 51, 53, 79, 108, and 127, with m/z 126 likely representing the molecular ion (C₆H₆O₃). Finally, β-D-Glucopyranose, 1,6-anhydro exhibits peaks at m/z 29, 31, 43, 57, and 73, with the m/z 57 peak indicating a key fragment. These spectra confirm the presence and fragmentation patterns of each compound, consistent with their molecular structures.

Table 8. Compounds identified in GC-MS analysis of the extract *Bergenia ciliata*

S. No.	R _T	Area%	m/z	Molecular formula	Compound	Structure
1	14.26	34.24	110	C ₆ H ₆ O ₂	Hydroquinone	
2	13.79	21.15	110	C ₆ H ₆ O ₂	Resorcinol	
3	15.51	20.84	128	C ₆ H ₆ O ₃	1,2,3-Benzenetriol	
4	17.69	14.42	162	C ₆ H ₁₀ O ₅	β-D-Glucopyranose, 1,6-anhydro	

Effective DNA isolation, PCR amplification, and sequencing for accurate species identification

The study successfully isolated high-quality DNA from plant tissue using the NucleoSpin® Plant II Kit, yielding sufficient and intact DNA suitable for further molecular analysis. The integrity and purity of the isolated DNA were confirmed by clear, distinct bands observed on a 0.8% agarose gel, indicating effective extraction without significant degradation. PCR amplification of the ITS region using ITS-F2 and ITS-R2 primers was successful, with electrophoresis on a 1.2% agarose gel showing clear bands at the expected size, confirming the target DNA fragment's successful amplification. Similarly, PCR amplification using RBCL-AF and RBCL-724R primers was also successful, producing clear bands of the expected size for the ITS region on the agarose gel, indicating effective target DNA amplification. The PCR products displayed distinct bands on a 1.2% agarose gel, verifying successful amplification and confirming the specificity of the primers used. Post-PCR, ExoSAP-IT treatment efficiently removed unwanted primers and dNTPs from the PCR product mixture, as indicated by the clean and sharp bands observed in subsequent sequencing steps, preparing the samples for accurate sequencing. High-quality sequences were obtained employing the BigDye Terminator v3.1 Cycle Sequencing Kit, with sequencing reactions producing clear and readable peaks, ensuring the acquisition of precise sequence data. The high quality of these sequences was confirmed utilizing Sequence Scanner Software v1, and subsequent alignment and editing utilizing Geneious Pro v5.1 enabled precise identification and comparison of the ITS sequences with those in

existing databases. This facilitated accurate species identification and assessment of genetic diversity, highlighting the effectiveness of the protocols used in this study for DNA isolation, amplification, and sequencing.

Relationships between taxa in terms of evolutionary approach using neighbor joining (NJ) approach with ITS gene sequences

The evolutionary history was inferred utilizing the Neighbor-Joining technique. The bootstrap consensus tree, which was produced from 500 replicates, is thought to indicate the evolutionary history of the taxa under investigation. Collapsed branches are indicative of divisions that are replicated in fewer than half of the bootstrap replicates. The proportion of replicate trees where related taxa clustered jointly in the bootstrap test (500 repetitions) is displayed next to the branches. The Jukes-Cantor method was utilized to compute the evolutionary gaps, which are given in base replacements per site. In this study, eight nucleotide sequences were examined. All ambiguous areas were eliminated for every pair of sequences. There were 729 places in the final dataset. To conduct evolutionary analysis, MEGA11 was utilized (Fig. 5).

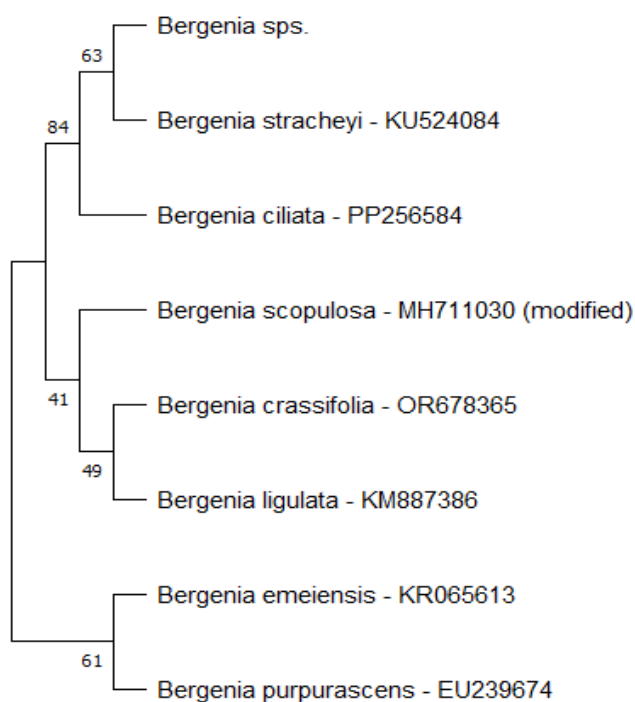


Figure 5. NJ Bootstrap tree ITS-2BR

Evolutionary analysis using the approach of maximum likelihood approach using rbcL gene sequences

To infer the evolutionary history, the Maximum Likelihood method and the Tamura 3-parameter model were employed. It is presumed that the bootstrap consensus tree, which was produced from 500 repetitions, represents the evolutionary history of the taxa under study. Partitions that are duplicated in less than 50% of bootstrap replicates are correlated with crumbled branches. Following the branches, one may find the percentage of replicate trees in which associated taxa were clustered jointly during the

500 bootstrap test repetitions. Employing the Neighbor-Join and BioNJ algorithms on a matrix of sequential gaps computed utilizing the Tamura 3 parameter model, the heuristic search's first tree or trees were automatically constructed. Afterwards, the topology with the largest log likelihood value was chosen. This study included seven different nucleotide sequences. In total, 640 positions were included in the final dataset. Evolutionary analysis was performed using MEGA11 (Fig. 6).

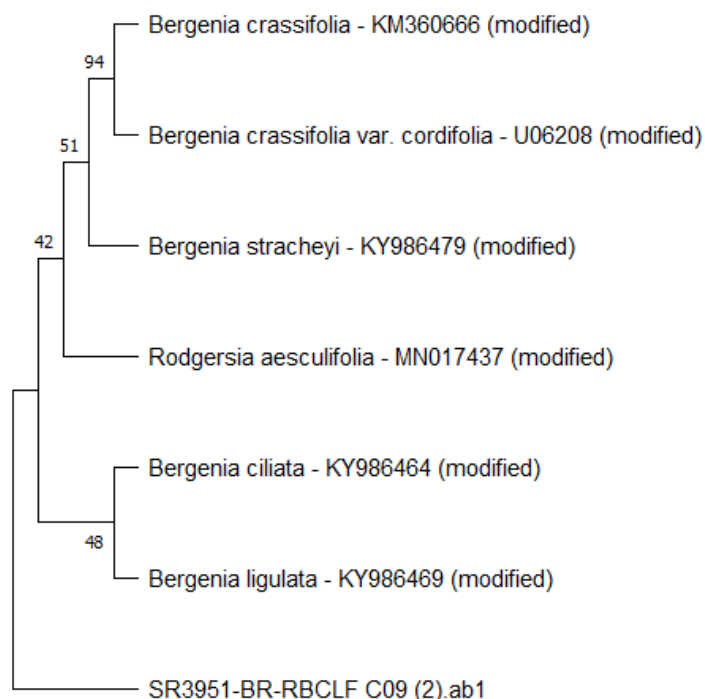


Figure 6. NJ bootstrap consensus tree

Discussion

A well-known species of *Bergenia* i.e. *Bergenia ligulata* is extensively used in traditional medicine in South Asia for their diuretic properties. Studies have shown the antioxidant potential of the *Bergenia* species using DPPH (Bashir and Gilani, 2009) and this study through the antioxidant activity as explained earlier showed promising antioxidant potential of *Bergenia Ciliata*. The dose-dependent antioxidant activity as measured through its free radical scavenging ability as elaborated in the earlier sections showed results that align with the earlier studies of antioxidant nature of the plant. As the concentration of the sample increases from 1.56 to 50 $\mu\text{g/mL}$, the percentage of scavenging activity rises significantly, starting at 7.96% and reaching 91.39% at the highest concentration. This activity is comparable to the standard antioxidant, ascorbic acid (C), which shows a scavenging activity of 92.44%. The IC₅₀ value, the concentration at which 50% of free radicals are scavenged, is calculated to be 17.8765 $\mu\text{g/mL}$, indicating that BR has potent antioxidant properties. This suggests that the plant, could be an effective natural antioxidant for use in health and food applications. Further the FTIR analysis during the study tried to find out molecules with varied functional groups which proved the content of phenolics and flavonoids in the plant material. The GCMS analysis led to the identification of four different molecules

as depicted in the results section in addition to already reported molecules like bergenin, catechin, gallic acid etc. (Dhalwal et al., 2008).

Wide spread studies across developing nations, with limited access to balanced diet are the reasons behind micronutrient malnutrition and that have long lasting impact on the health of the individuals affecting morbidity and mortality (Rautiainen et al., 2016). The proximate analysis and mineral element analysis during the study produced sufficient results to support that the plant can be a good and an alternative source of food. With further standardization and calibration it could be a good nutraceutical to overcome diseases due to deficiency of essential mineral element. Further with its antimicrobial potential against range of microbes as explained in the results the plant can be used as an alternative to preservatives for the storage of food products for longer shelf life. This will make the product more acceptable in the consumer market due to low content of chemical preservatives.

The current state in the nutraceutical or traditional medicine is that, plant-based formulations were found to be contaminated and adulterated with impurities (Ichim and Booker, 2021). Despite of regulations, such products still find their way in to the market and reach to consumers which adversely impact their health. One of the best methods to determine adulterants at micro level, standard DNA barcodes were found to be effective tools (Mishra et al., 2016). The current study used two standard DNA barcodes for the identification of the plant material i.e. *ITS* and *rbcl*. At first, *ITS* sequences were taken into consideration. The region is sequenced, and retrieval of 7-8 sequences from gene bank with more than 90% similarity index and then tree formation using MEGA11. The tree showed 63% bootstrap value in a single clad with *Bergenia stracheyi* and no out group formation was found which is depicted in *Figure 5* under results section. Similarly, while using *rbcl* sequences the same procedure was followed and found that *rbcl* forms an outgroup with no common clad with any known retrieved sequences from NCBI gene bank as shown in *Figure 6*. This can be concluded that *ITS* could be a better DNA barcode as compared to *rbcl* while testing any material with the plant under study as one of the constituent substances.

The study therefore, gives a broader understanding of the diverse properties the plant material have in terms of proximate, antimicrobial, antioxidant and mineral element content. It further provides a way forward for the identification of the plant, if it is used as a formulation in nutraceutical or in traditional medicine setup.

Conclusion

The study comprehensively characterized the endangered medicinal plant *Bergenia ciliata* through a multifaceted approach. DNA barcoding ensured accurate species identification, paving the way for detailed chemical analysis. ICP-MS, FTIR, and GC-MS revealed the plant's elemental composition, functional groups, and specific compounds, respectively. The presence of antimicrobial properties was confirmed. Furthermore, in addition to its known traditional values this study elaborated the nutritive value of the plant. Future studies are needed to explore the content of heavy metals, proper dosage concentrations for effectiveness and exact identification of the plant via metabarcoding. These findings underscore the significant medicinal potential of *B. ciliata* and emphasize the importance of integrated research methodologies for exploring these plants for medicine and as food supplements, but a check should be there to avoid overexploitation of these valuable resources.

Conflict of interests. The authors declare no conflict of interests in relation to this article

REFERENCES

- [1] Adetunji, T. L., Padi, P. M., Olawale, F., Mchunu, C. N., Ntuli, N. R., Siebert, F. (2023): Nutraceutical evaluation of *Evolvulus alsinoides* L. (L.), a browse species collected from the wild around Selwane village, Limpopo Province, South Africa. – *South African Journal of Botany* 157: 243-250.
- [2] Álvarez, I., Wendel, J. F. (2003): Ribosomal ITS sequences and plant phylogenetic inference. – *Molecular Phylogenetics and Evolution* 29(3): 417-434.
- [3] Arceusz, A., Radecka, I., Wesolowski, M. (2010): Identification of diversity in elements content in medicinal plants belonging to different plant families. – *Food Chemistry* 120(1): 52-58.
- [4] Bahukhandi, A., Sekar, K. C., Barola, A., Bisht, M., Mehta, P. (2019): Total phenolic content and antioxidant activity of *Meconopsis aculeata* Royle: a high value medicinal herb of Himalaya. – *India Section B: Biological Sciences* 89: 1327-1334.
- [5] Bashir, S., Gilani, A. H. (2009): Antiurolithic effect of *Bergenia ligulata* rhizome: an explanation of the underlying mechanisms. – *Journal of Ethnopharmacology* 122(1): 106-116.
- [6] Bathe, G. A., Patil, V. S., Chaurasia, A. S. (2012): Study on temperature gradients and protein enrichment by *Aspergillus oryzae* in solid-state fermentation on packed bed bioreactor using Jowar (sorghum) straw as substrate. – *Journal of Sustainable Bioenergy Systems* 2(3): 33.
- [7] Chase, M. W., Fay, M. F. (2009): Barcoding of plants and fungi. – *Science* 325(5941): 682-683.
- [8] Dhalwal, K., Shinde, V. M., Biradar, Y. S., Mahadik, K. R. (2008): Simultaneous quantification of bergenin, catechin, and gallic acid from *Bergenia ciliata* and *Bergenia ligulata* by using thin-layer chromatography. – *Journal of Food Composition and Analysis* 21(6): 496-500.
- [9] Ding, Y., Jiang, G., Huang, L., Chen, C., Sun, J., Zhu, C. (2020): DNA barcoding coupled with high-resolution melting analysis for nut species and walnut milk beverage authentication. – *Journal of the Science of Food and Agriculture* 100(6): 2372-2379.
- [10] Gill, B. A., Musili, P. M., Kurukura, S., Hassan, A. A., Goheen, J. R., Kress, W. J., Kuzmina, M., Pringle, R. M., Kartzinel, T. R. (2019): Plant DNA-barcode library and community phylogeny for a semi-arid east African savanna. – *Molecular Ecology Resources* 19(4): 838-846.
- [11] Gregory, T. R. (2005): DNA barcoding does not compete with taxonomy. – *Nature* 434(7037): 1067-1067.
- [12] Han, J., Pang, X., Liao, B., Yao, H., Song, J., Chen, S. (2016): An authenticity survey of herbal medicines from markets in China using DNA barcoding. – *Scientific Reports* 6(1): 18723.
- [13] Hollingsworth, P. M., Graham, S. W., Little, D. P. (2011): Choosing and using a plant DNA barcode. – *PloS ONE* 6(5): e19254.
- [14] Ichim, M. C., Booker, A. (2021): Chemical authentication of botanical ingredients: a review of commercial herbal products. – *Frontiers in Pharmacology* 12: 666850.
- [15] Islam, S. U., Dar, T. U., Khuroo, A. A., Bhat, B. A., Mangral, Z. A., Tariq, L., Tantray, W. W., Malik, A. H. (2021): DNA barcoding aids in identification of adulterants of *Trillium govanianum* wall. Ex d. Don. – *Journal of Applied Research on Medicinal and Aromatic Plants* 23: 100305.
- [16] Jamshidi-Kia, F., Lorigooini, Z., Amini-Khoei, H. (2017): Medicinal plants: past history and future perspective. – *Journal of Herbmmed Pharmacology* 7(1): 1-7.

- [17] Jamwal, M., Puri, S., Sharma, N., Prakash, S., Pundir, A. (2023): Altitudinal variation in phytochemical, physicochemical, and morphological aspects of *Justicia adhatoda* L. plant growing wildly in Western Himalayas. – *Journal of Applied Biology and Biotechnology* 11(3): 85-96.
- [18] Kress, W. J., Wurdack, K. J., Zimmer, E. A., Weigt, L. A., Janzen, D. H. (2005): Use of DNA barcodes to identify flowering plants. – *Proceedings of the National Academy of Sciences* 102(23): 8369-8374.
- [19] Kumar, R., Joshi, R., Kumar, R., Srivatsan, V., Satyakam, Chawla, A., Patial, V., Kumar, S. (2022): Nutritional quality evaluation and proteome profile of forage species of Western Himalaya. – *Grassland Science* 68(3): 214-225.
- [20] Li, S., Han, Q., Qiao, C., Song, J., Lung Cheng, C., Xu, H. (2008): Chemical markers for the quality control of herbal medicines: an overview. – *Chinese Medicine* 3: 1-16.
- [21] Mishra, P., Kumar, A., Nagireddy, A., Mani, D. N., Shukla, A. K., Tiwari, R., Sundaresan, V. (2016): DNA barcoding: An efficient tool to overcome authentication challenges in the herbal market. – *Plant Biotechnology Journal* 14(1): 8-21.
- [22] Nithaniyal, S., Vassou, S. L., Poovitha, S., Raju, B., Parani, M. (2017): Identification of species adulteration in traded medicinal plant raw drugs using DNA barcoding. – *Genome* 60(2): 139-146.
- [23] Radha, Kumar, M., Puri, S., Pundir, A., Bangar, S. P., Changan, S., Choudhary, P., Parameswari, E., Alhariri, A., Samota, M. K., Damale, R. D., Singh, S., Berwal, M. K., Dhumal, S., Bhoite, A. K. G., Senapathy, M., Sharma, A., Bhushan, B., Mekhemar, M (2021): Evaluation of nutritional, phytochemical, and mineral composition of selected medicinal plants for therapeutic uses from cold desert of Western Himalaya. – *Plants* 10(7): 1429.
- [24] Rasul, M. G. (2018): Extraction, isolation and characterization of natural products from medicinal plants. – *International Journal of Basic Sciences and Applied Computing* 2(6): F0076122618.
- [25] Rautiainen, S., Manson, J. E., Lichtenstein, A. H., Sesso, H. D. (2016): Dietary supplements and disease prevention—a global overview. – *Nature Reviews Endocrinology* 12(7): 407-420.
- [26] Salmerón-Manzano, E., Garrido-Cardenas, J. A., Manzano-Agugliaro, F. (2020): Worldwide research trends on medicinal plants. – *Int J Environ Res Public Health* 17(10): 3376.
- [27] Sarma, N. D., Waye, A., ElSohly, M. A., Brown, P. N., Elzinga, S., Johnson, H. E., MarlesMelanson, J. E., Russo, E., Deyton, L., Hudalla, C., Vrdoljak, G. A., Wurzer, J. H., Khan, I. A., Kim, N. C., Giancaspro, G. I. (2020): Cannabis inflorescence for medical purposes: USP considerations for quality attributes. – *Journal of Natural Products* 83(4): 1334-1351.
- [28] Shah, H., Naseer, A., Gupta, N., Patil, S., Upadhyay, S. K., Singh, R. (2021): Proximate analysis and phytochemistry of different plant parts of *Myrica esculenta* extracts. – *Plant Cell Biotechnology and Molecular Biology* 22(55&56): 90-102.
- [29] Sharma, D., Bhandari, T., Pradhan, A., Ghimire, N., Basnet, S., Pandey, S., Lamichhane, J. (2020): DNA barcoding, phytochemical screening and antimicrobial activity of *rhododendron arboreum*, a high altitudinal medicinal plant from Nepal. – *Eurasian Journal of Forest Science* 8(2): 140-151.
- [30] Shin, J. M., Park, S. K. (2015): Comparison of fat determination methods depending on fat definition in bakery products. – *LWT-Food Science and Technology* 63(2): 972-977.
- [31] Thakur, A., Singh, S., Dulta, K., Singh, N., Ali, B., Hafeez, A., Vodnar, D. C., Marc, R. A. (2022): Nutritional evaluation, phytochemical makeup, antibacterial and antioxidant properties of wild plants utilized as food by the gaddis-a tribal tribe in the Western Himalayas. – *Frontiers in Agronomy* 4: 1010309.

- [32] Vashistha, R. K., Butola, J. S., Nautiyal, B., Nautiyal, M. C. (2010): Phenological attributes of *Angelica glauca* and *A. archangelica* expressed at two different climatic zones in Western Himalaya. – *Journal of Medicinal and Aromatic Plants* 1(1): 7-12.
- [33] Yemm, E., Willis, A. J. (1954): The estimation of carbohydrates in plant extracts by anthrone. – *Biochemical Journal* 57(3): 508.
- [34] Yu, M., Gouvinhas, I., Rocha, J., Barros, A. I. (2021): Phytochemical and antioxidant analysis of medicinal and food plants towards bioactive food and pharmaceutical resources. – *Scientific Reports* 11(1): 10041.

APPENDIX

Yield from Soxhlet extraction

Determination of extraction yield

The extraction yield (%) was calculated as follows:

= weight of extract after evaporation solvent and freeze drying / dry weight of the sample $\times 100$

S.No.	Sample code	Weight used for extraction (g)	Extract weight after drying solvent (g)	Yield (%)
1.	BRL	25	0.751	7.51

Protein content

S.No.	Sample code	Replicates	Wt	Titrant volume (V1)	Nitrogen (%)	Crude protein (%)	Mean \pm SD
1	BRL	R1	2.044	1.5	0.103	5.859	6.407 \pm 0.475
2		R2	2.032	1.7	0.117	6.680	
3		R3	2.031	1.7	0.117	6.683	

Moisture content

Table showing the values and calculations for the % moisture content of the sample

S.No.	Sample code	Replicates	Wt of dish	Wt of dish + sample (before drying)	Wet wt of sample	Wt of dish + sample (after drying)	Moisture content (%)	Mean \pm SD
1	BRL	R1	34.670	36.648	1.978	36.390	12.900	12.917 \pm 0.925
2		R2	36.340	38.340	2.000	38.100	12.000	
3		R3	34.640	36.648	2.008	36.371	13.850	

Crude fiber content

Table showing the values and calculations for the crude fiber content of the sample

S.No.	Sample code	Replicates	Wt. of crucible	W1	W2	W3	Crude fiber (%)	Mean \pm SD
1	BRL	R1	27.317	0.261	0.075	5.017	3.709	4.199 \pm 0.893
2		R2	27.328	0.338	0.075	5.026	5.230	
3		R3	27.347	0.247	0.063	5.047	3.658	

Crude fat content

Table showing the values and calculations for the crude fat content

S.No.	Sample code	Replicates	W2	W1	WS	Crude fat (%)	Mean ± SD
1	BRL	R1	122.300	122.312	0.012	0.593	0.611 ± 0.071
2		R2	122.310	122.321	0.011	0.550	
3		R3	122.300	122.314	0.014	0.689	

Ash content

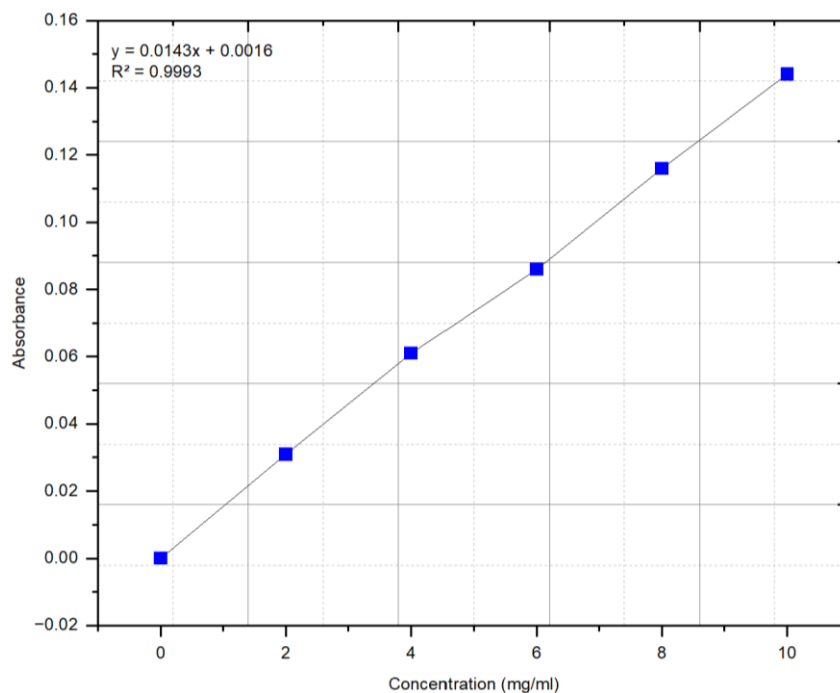
Table showing the values and calculations for the % ash content

S.No.	Sample code	Replicates	Weight of crucible	Weight of sample with crucible	Weight of sample (g)	After ashing weight	Weight of ash (g)	Ash content (%)	Mean ± SD
1	BRL	R1	27.330	29.330	2.000	27.430	0.100	5.000	4.618 ± 0.641
2		R2	26.780	28.790	2.010	26.880	0.100	4.975	
3		R3	27.340	29.145	1.805	27.410	0.070	3.878	

Carbohydrate content

Table showing the values and calculations for the carbohydrate content in mg/ml

S.No.	Concentration (mg/ml)	Absorbance
1	0	0
2	2	0.031
3	4	0.061
4	6	0.086
5	8	0.116
6	10	0.144



S.No.	Sample code	Absorbance	Concentration (mg/ml)	Mean \pm SD
1	BRL	0.93	64.923	64.457 \pm 0.807
		0.91	63.524	
		0.93	64.923	

GC MS mass spectra

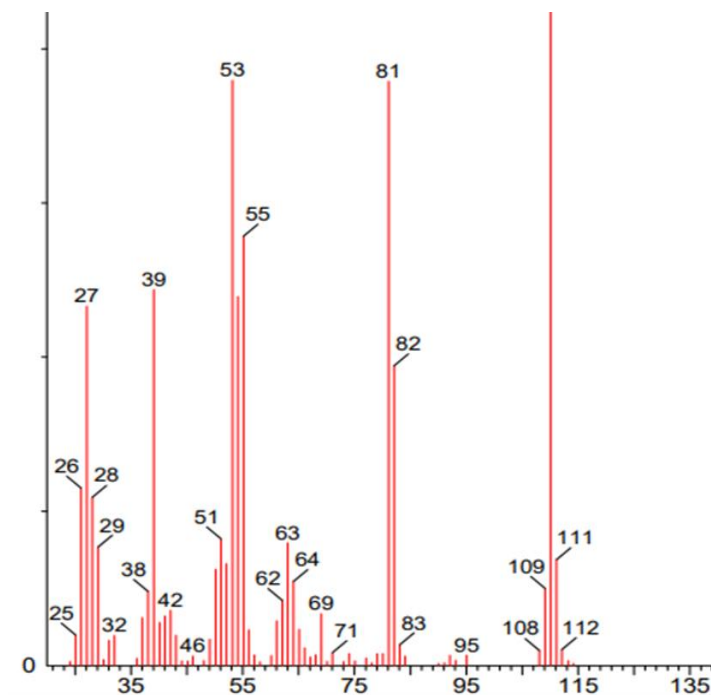


Figure A1. GC-MS analysis of the sample with compound hydroquinone

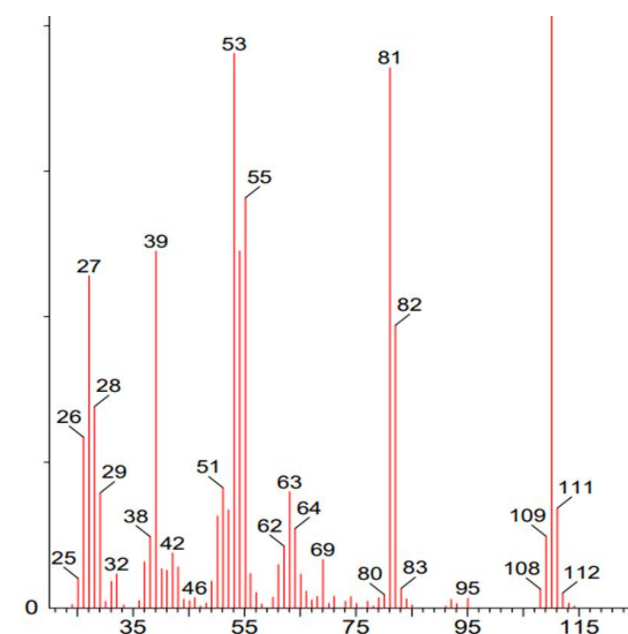


Figure A2. GC-MS analysis of the sample with compound resorcinol

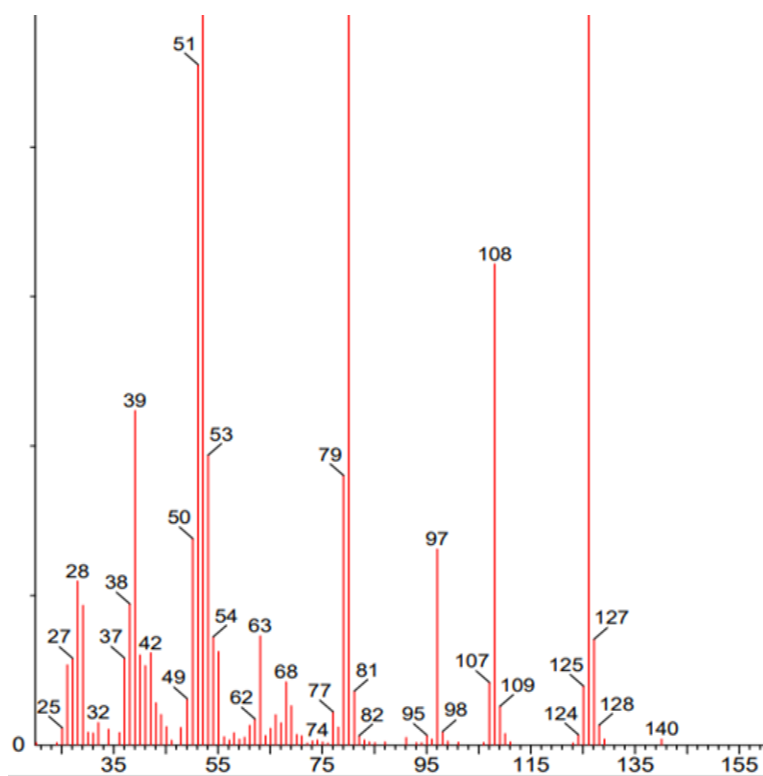


Figure A3. GC-MS analysis of the sample with compound 1,2,3-benzenetriol

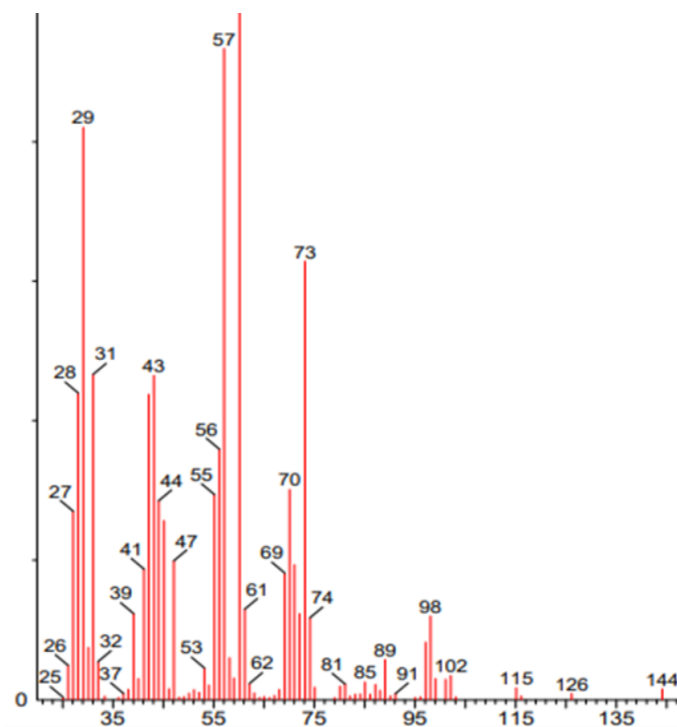


Figure A4. GC-MS analysis of the sample with compound β -D-glucopyranose, 1,6-anhydro